

Scientific Report No. 50

TOTAL AND PARTIAL REFLECTION FROM THE END OF A PARALLEL
PLATE WAVEGUIDE WITH AN EXTENDED DIELECTRIC SLAB*

by

David C. Chang and Edward F. Kuester

December 1979

Electromagnetics Laboratory
Department of Electrical Engineering
University of Colorado
Boulder, Colorado 80309

*This work is supported by NSF under Grant No. 7809029.
Dr. E. Schutzman is the Program Monitor.

TABLE OF CONTENTS

Abstract

1. Introduction	1
2. Scattered and Reflected Fields for a TEM Incidence	2
3. Spectral Solution $\tilde{F}_-(\lambda)$ and $\tilde{G}_-(\lambda)$	11
4. Reflection Coefficient and End Admittance	14
5. Far Field and Surface-wave Radiation	18
6. Numerical Examples	23
References	25
Appendix A	A-1
Appendix B	B-1
Appendix C	C-1

TOTAL AND PARTIAL REFLECTION FROM THE END OF A PARALLEL-PLATE
WAVEGUIDE WITH AN EXTENDED DIELECTRIC SLAB

by

David C. Chang and Edward F. Kuester
Electromagnetics Laboratory
Department of Electrical Engineering
University of Colorado
Boulder, Colorado 80309

Abstract

This investigation concerns a TEM wave incident obliquely onto the opening of a parallel plate waveguide with a truncated upper plate. The lower plate as well as the dielectric slab, between the two plates, are assumed to be extended out indefinitely in order to support the propagation of at least one surface wave mode. Reflection from the waveguide opening is determined as a function of incident angle via a dual Wiener-Hopf formulation. It is found that a total reflection, i.e., the magnitude of the reflection coefficient equals to unity, is possible for incident angles greater than the critical angle associated with the lowest-order surface-wave mode of the grounded dielectric slab. The field external to the parallel plate waveguide in this case becomes completely evanescent in the cross-sectional plane perpendicular to the plane of incidence, which is determined by the propagation direction of the incident wave and the edge of the upper plate. It is shown that the phase of the reflection coefficient thus obtained can be used to construct the modal equation for the fundamental mode(s) of a wide microstrip.

TOTAL AND PARTIAL REFLECTION FROM THE END OF A PARALLEL-PLATE WAVEGUIDE WITH AN EXTENDED DIELECTRIC SLAB

1. Introduction

The problem of a truncated parallel-plate waveguide with an opening onto a grounded dielectric slab extended from the waveguide region has been widely investigated, mainly because it provides an understanding on the launching of surface-wave modes on the slab structures [Angulo and Chang, Bates and Mittra 1968, Fong, 1972, Zhurov 1975]. Since efficient excitation of the surface waves is the central issue, most of the effort has been expended in investigating the case of normal incidence of individual modes in the parallel-plate region. More recently, question of the reflection of a TEM-wave from a dielectric slab which is not thick enough to support any well-confined surface-wave mode has received particular attention because the structure is closely related to that of a microstrip. It is recognized by Fong and Lee [1971], and recently by Fialkoskii and his colleagues [1977] that a truncated parallel-plate in the presence of a grounded dielectric slab forms a canonical problem for studying the quasi-TEM as well as other higher order modes guided by the structure. Mathematically, the problem becomes much more complicated than the normal incidence case however, due to the fact that both LSE-wave and LSM-wave, characterized respectively by the electric and the magnetic field component normal to the slab surface, can be excited by the TEM-wave with a general incidence angle. Also because the interest now is to study guided modes, solutions that exhibit an exponentially-decaying behavior in a cross-sectional plane are those warranting particular attention. Only lately with the development of microstrip antennas, does the problem of understanding the governing relationship for waveguiding and wave radiation become more important.

In this paper, the canonical problem of a grounded slab with a truncated upper plate is treated analytically in detail. Expressions for the reflection coefficient and end admittance are derived. Numerical examples pertaining to both waveguiding characteristics and radiation characteristics of the structure are also given.

2. Scattered and Reflected Fields for a TEM Incidence

Consider the problem of a semi-infinite, perfectly conducting half-plane placed in the interface between air and a grounded slab of thickness d , as depicted in Figure 1. The slab is assumed to be lossless, having a relative permittivity ϵ_r and permeability μ_r . A TEM-wave of unit amplitude is incident obliquely in the parallel plate region between the conducting strip and the ground at an angle ϕ with respect to the y -axis. Defining $\alpha = n \sin \phi$ where $n = (\mu_r \epsilon_r)^{\frac{1}{2}}$ is the refractive index of the slab, the field components associated with this incident field can be written as

$$\begin{cases} E_z^i = \exp\{-ik_0[\alpha x - (n^2 - \alpha^2)^{\frac{1}{2}} y]\} \\ \bar{H}_t^i = -(\mu_r \eta_0)^{-1} [\bar{a}_x (n^2 - \alpha^2)^{\frac{1}{2}} + \bar{a}_y \alpha] \exp\{-ik_0[\alpha x - (n^2 - \alpha^2)^{\frac{1}{2}} y]\} \end{cases} \quad (1)$$

with a suppressed time-factor of $\exp(i\omega t)$; $k_0 = \omega(\mu_0 \epsilon_0)^{\frac{1}{2}}$ is the free-space wave number, $\eta_0 = (\mu_0 / \epsilon_0)^{\frac{1}{2}} = 120\pi$ ohms; \bar{a}_x and \bar{a}_y are the unit vectors in the x - and y - direction. To find the reflection as well as radiation of this wave, we shall derive later in this section, a spectrum-domain formulation which allows us to find the solution via the classical Wiener-Hopf technique. Before we can do that however, some comments must be made regarding the physical nature of the problem.

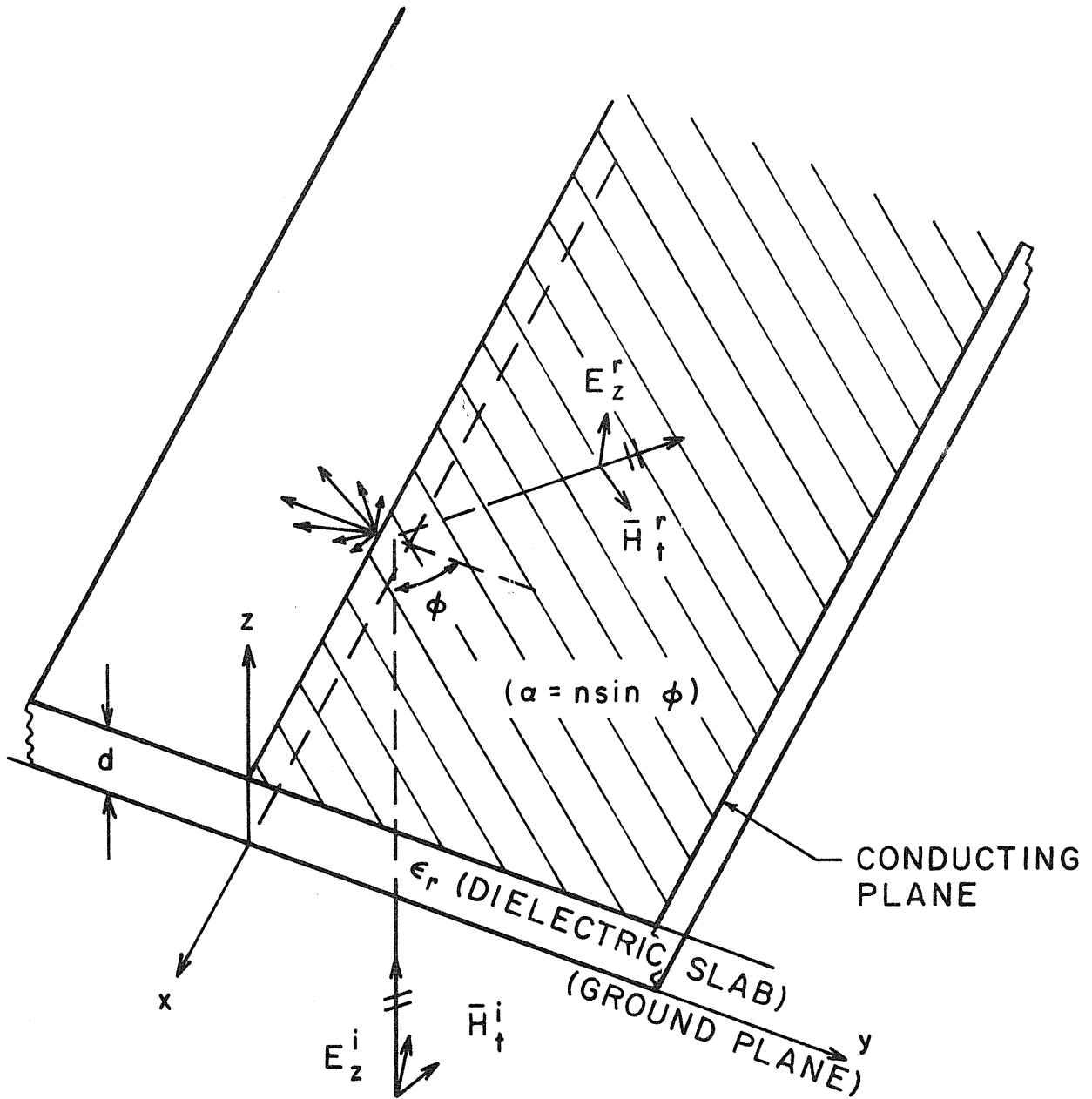


Figure 1

As it is well-known in the theory of surface waves, a grounded dielectric slab in the absence of the conducting strip can support a finite number of surface-waves --the exact number of which depends upon the so-called "numerical aperture" defined as $V = (\mu_r \epsilon_r - 1)^{\frac{1}{2}} k_0 d$ of the structure. Among these, the LSE₁-mode with the electric field polarized in the z-direction actually has no cut-off. Thus, one would at least expect the excitation of this wave as a direct result of the TEM-wave incidence. However, unlike a two-dimensional problem where one assumes no variation in the x-direction, both the surface-wave and the radiation field in the open region can propagate in one direction, while exponentially decay in another direction. For instance, since the total solution has to have the same variation of $\exp(-ik_0 \alpha x)$ along the x-direction as the incident wave, the far-field observed at a fixed elevation angle θ in any cross-section has to behave like $f(\theta) \exp(ik_0 [1-\alpha^2]^{\frac{1}{2}} r)$ in air where r is the radial-distance from the parallel-strip waveguide opening. Depending upon the incident wave, the quality $\alpha = n \sin \phi$ can vary from 0 to n . Therefore, for $\alpha < 1$, the "scattered" field indeed propagates radially away from the waveguide opening, but for $1 < \alpha < n$, the scattered field decays exponentially instead. In a very similar fashion, the field components associated with a surface-wave of wave number α_p must behave like $\exp[-k_0 (\alpha_p^2 - 1)z] \exp\{-ik_0 [\alpha x - (\alpha_p^2 - \alpha^2)^{\frac{1}{2}} y]\}$ in air. Thus, for $\alpha_p < \alpha < n$, an exponential decay of field in both y and z direction, is again observed. We note that the value of α_p is determined from

$$\epsilon_r (\alpha_p^2 - 1)^{\frac{1}{2}} = (n^2 - \alpha_p^2)^{\frac{1}{2}} \tan[(n^2 - \alpha_p^2)^{\frac{1}{2}} k_0 d] \quad (2)$$

for a LSE surface-wave, and from

$$\mu_r (\alpha_p^2 - 1)^{\frac{1}{2}} = (n^2 - \alpha_p^2)^{\frac{1}{2}} \cot[(n^2 - \alpha_p^2)^{\frac{1}{2}} k_0 d] \quad (3)$$

for LSM surface-waves (if they exist).

The above discussion points to a very important feature, unique to the study of oblique incidence. That is, whether the opening at the end, i.e. $y = 0$, will actually allow the TEM-wave in the parallel plate region to radiate into the open-space or not depends upon the angle of the incident wave. A complete reflection of the wave is therefore entirely possible, if the angle of incidence $\phi = \sin^{-1}(\alpha/n)$ is greater than some critical angle $\phi_c = \sin^{-1}(\alpha_{p,\max}/n)$ where $\alpha_{p,\max}$ is obtained from the surface-wave mode having the largest value of α_p . Such a phenomenon is certainly not unlike a plane-wave incident obliquely from a lossless medium having a large refractive index to a medium with a smaller refractive index. Reflection coefficient of the TEM-wave in this case can be expressed in the form $\Gamma_{\text{TEM}} = \exp[+i\chi(\alpha)]$ so that the magnitude is of unity. It is of interest to note that, for a conducting strip of finite width ℓ , the total phase change for a TEM-wave bouncing back and forth once between the two ends of the strip is $2\chi - 2k_0(n^2 - \alpha^2)^{\frac{1}{2}}\ell$, provided the field diffracted from one end will not be significantly coupled into the other end. Thus a transverse resonance can be achieved if and when the total phase change equals integer multiples of 2π :

$$2\chi(\alpha) - 2k_0(n^2 - \alpha^2)^{\frac{1}{2}}\ell = 2m\pi; \quad m = 0, 1, 2 \dots \quad (4)$$

The particular values of α , $m = 0, 1, 2 \dots$ that produce this resonance then correspond to the propagating modes of a microstrip structure. Of course, because α has to be less than n for a TEM-wave under the strip one expects only a finite number of acceptable α_m , most likely one, that will produce this resonance. In a companion paper, we shall expand this viewpoint and show that equation (4) provides the correct dispersion relationship for the quasi-TEM mode and higher-order modes of a wide microstrip problem.

We now proceed to formulate the spectral-domain representation of the scattered field. Defining a Fourier transform pair;

$$\begin{cases} \tilde{f}(\lambda) = \frac{k_0}{2\pi} \left(\int_{-\infty}^0 + \int_0^{\infty} \right) f(y) e^{ik_0 \lambda y} dy = \tilde{f}_-(\lambda) + \tilde{f}_+(\lambda) \\ f(y) = \int_{-\infty}^{\infty} \tilde{f}(\lambda) e^{-ik_0 \lambda y} d\lambda \end{cases} \quad (5)$$

where \tilde{f}_+ , \tilde{f}_- are defined, respectively, as the integration from 0 to ∞

and from $-\infty$ to 0. Provided that $f(y)$ corresponds to a physically realizable function, one can define an arbitrarily small positive number, τ_0 and

show that $\tilde{f}_+(\lambda)$ is analytic in the upper half of the λ -plane, i.e.

$\text{Im } \lambda \geq -\tau_0$, and $\tilde{f}_-(\lambda)$ is analytic in the lower half, i.e. $\text{Im } \lambda < \tau_0$ (Fig.2).

Now since the scattered field has to vary along x like $\exp(ik_0 \alpha x)$ as the incidence field does, its spectral representation in the air region, $z > d$, can be shown to be

$$\begin{aligned} \tilde{E}_z^S &= E_0 e^{-u_0 k_0 (z-d)} ; \quad \tilde{H}_z^S = H_0 e^{-u_0 k_0 (z-d)} \\ \tilde{E}_t^S &= \frac{i}{\alpha^2 + \lambda^2} [(\alpha \bar{a}_x + \lambda \bar{a}_y) u_0 E_0 e^{-u_0 k_0 (z-d)} - i \eta_0 (\alpha \bar{a}_y - \lambda \bar{a}_x) H_0 e^{-u_0 k_0 (z-d)}] \\ \tilde{H}_t^S &= \frac{i}{\alpha^2 + \lambda^2} [(\alpha \bar{a}_x + \lambda \bar{a}_y) u_0 H_0 e^{-u_0 k_0 (z-d)} + i \eta_0^{-1} (\alpha \bar{a}_y - \lambda \bar{a}_x) E_0 e^{-u_0 k_0 (z-d)}] \end{aligned} \quad (6)$$

where $u_0 = (\lambda^2 + \alpha^2 - 1)^{\frac{1}{2}}$; $\text{Re } u_0 \geq 0$, and (E_0, H_0) are two yet undetermined functions of λ . In what follows, the explicit dependence on x , i.e. $\exp(ik_0 x)$ will be suppressed. Similarly, in the slab region, $z < d$,

$$\tilde{E}_z^S = E_n \frac{\text{ch } u_n k_0 z}{\text{ch } u_n k_0 d} ; \quad \tilde{H}_z^S = H_n \frac{\text{sh } u_n k_0 z}{\text{sh } u_n k_0 d} ,$$

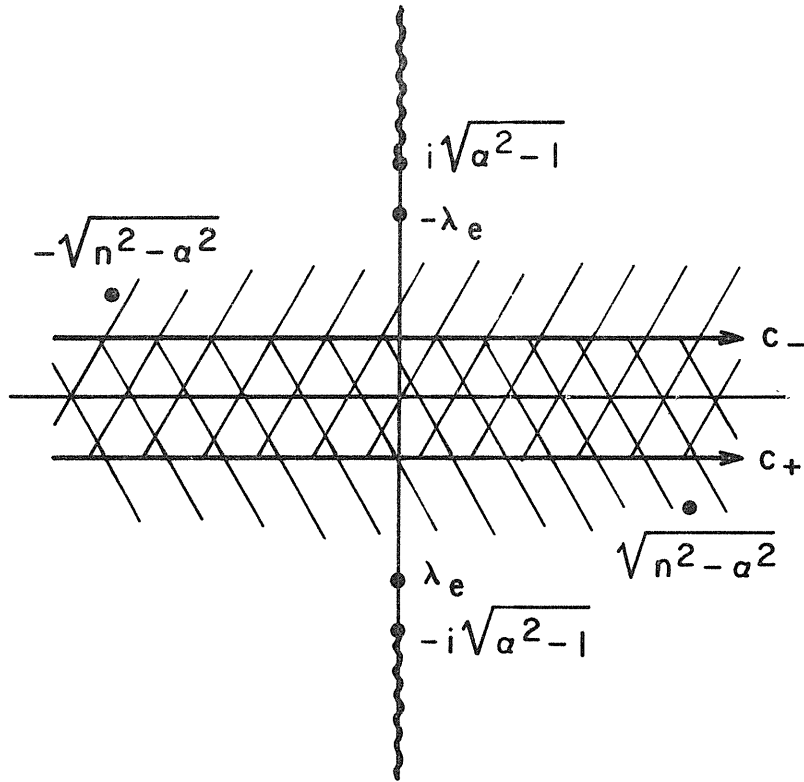


Figure 2

$$\tilde{E}_t^S = \frac{i}{\alpha^2 + \lambda^2} [-(\alpha \bar{a}_x + \lambda \bar{a}_y) \left(\frac{u_n \text{sh } u_n k_o z}{\text{ch } u_n k_o d} \right) E_n - i \eta_o \mu_r (\alpha \bar{a}_y - \lambda \bar{a}_x) \left(\frac{\text{sh } u_n k_o z}{\text{sh } u_n k_o d} \right) H_n] \quad (7)$$

$$\tilde{H}_t^S = \frac{i}{\alpha^2 + \lambda^2} [-(\alpha \bar{a}_x + \lambda \bar{a}_y) \left(\frac{u_n \text{ch } u_n k_o z}{\text{sh } u_n k_o d} \right) H_n + i \eta_o^{-1} \epsilon_r (\alpha \bar{a}_y - \lambda \bar{a}_x) \left(\frac{\text{ch } u_n k_o z}{\text{ch } u_n k_o d} \right) E_n]$$

where $u_n = (\lambda^2 + \alpha^2 - n^2)^{\frac{1}{2}}$. Again, (E_n, H_n) are two yet undetermined functions of λ . Since the incident electric field has no tangential component, the continuity condition, $\tilde{E}_t^S(d+0) = \tilde{E}_t^S(d-0)$ yields immediately,

$$H_o = \mu_r H_n, \quad u_o E_o = -(u_n \text{th } u_n k_o d) E_n \quad (8)$$

We note that the scattered field is given in (6) and (7) in terms of a representation in LSE and LSM modes.

Before we proceed to determine the remaining two constants, we first define $\tilde{F}_-(\lambda)$ and $\tilde{G}_-(\lambda)$ as the Fourier transforms of the quantities $\nabla_t \cdot \bar{E}_t^S/k_o$ and $\bar{a}_z \cdot \nabla_t \times \bar{E}_t^S/k_o$, in the interface, $z = d$. Here, ∇_t is the "del" operator in the plane transverse to z , and \bar{a}_z is the unit vector in the direction of z . Because both $\nabla_t \cdot \bar{E}_t^S$ and $\bar{a}_z \cdot \nabla_t \times \bar{E}_t^S$ vanish on the conducting strip, it is clear that

$$\begin{aligned} \tilde{F}_-(\lambda) &= \frac{1}{2\pi} \int_{-\infty}^0 \nabla_t \cdot \bar{E}_t^S(y;d) e^{ik_o \lambda y} dy; \\ \tilde{G}_-(\lambda) &= \frac{1}{2\pi} \int_{-\infty}^0 \bar{a}_z \cdot \nabla_t \times \bar{E}_t^S(y;d) e^{ik_o \lambda y} dy \end{aligned} \quad (9)$$

are "negative" functions, analytic only in the lower half of the complex λ -plane.

Applying the definitions in (9), one sees immediately from (6) that both E_o and H_o are expressible in terms of \tilde{F}_- and \tilde{G}_- :

$$E_o = \tilde{F}_-(\lambda)/u_o; \quad H_o = i \eta_o^{-1} \tilde{G}_-(\lambda)$$

or

$$E_n = -(u_n \text{th } u_n k_o d)^{-1} \tilde{F}_-(\lambda) ; \quad H_n = i(\mu_r \eta_o)^{-1} \tilde{G}_-(\lambda) \quad (10)$$

As shown in Appendix A, a Wiener Hopf formulation for $F_-(\lambda)$ can be derived by imposing the boundary condition that the total normal electric flux is continuous at the air-slab interface, i.e.

$$\epsilon_r E_Z^S(y; d-0) + \epsilon_r E_Z^i(y; d-0) = E_Z^S(y; d+0), \quad \text{for } y < 0$$

and that the scattered component is discontinuous by the amount equal to the induced charge density on the metallic strip, i.e. $E_Z^S(y; d+0) - \epsilon_r E_Z^S(y; d-0) = \rho^S(y)$, for $y \geq 0$. Defining $\tilde{\rho}_+^S$ as the Fourier transform of ρ^S , we obtain from (A.2) the following Wiener Hopf equation

$$\tilde{F}_-(\lambda) = Q_e(\lambda) [\tilde{\rho}_+^S(\lambda) - \tilde{\rho}_-^i(\lambda)] / \epsilon_o \quad (11)$$

where

$$Q_e(\lambda) = \frac{u_o u_n \text{th } u_n k_o d}{\epsilon_r u_o + u_n \text{th } u_n k_o d} \quad (12)$$

and

$$\begin{aligned} \tilde{\rho}_-^i(\lambda) &= \frac{-k_o \epsilon_o}{2\pi} \int_0^{\infty} \epsilon_r E_Z^i(y; d-0) e^{ik_o \lambda y} dy \\ &= \left(\frac{i \epsilon_r \epsilon_o}{2\pi} \right)^{-\infty} \left[\frac{1}{\lambda + (n^2 - \alpha^2)^{\frac{1}{2}}} \right]_- \end{aligned} \quad (13)$$

is the Fourier transform of the charge density of the incident TEM-wave on the strip. Since $\tilde{\rho}_+^S$ and $\tilde{\rho}_-^i$ is obtained by integrating, respectively, ρ^S from 0 to ∞ and ρ^i from $-\infty$ to 0, the (\pm) signs account for the different regions of analyticity associated with them. Likewise, a Wiener-Hopf equation for \tilde{G}_- can be obtained by imposing the suitable boundary condition for the normal magnetic field at the interface. As shown in eq. (A.5) in Appendix A, one obtains the following:

$$i\omega\epsilon_0 \tilde{G}_-(\lambda) = Q_m(\lambda) \tilde{j}_+(\lambda) \quad (14)$$

where

$$Q_m(\lambda) = \frac{\mu_r}{\mu_r u_0 + u_n \operatorname{cth} u_n k_0 d}, \quad (15)$$

and $\tilde{j}_+(\lambda)$ is defined as the Fourier transform of $\bar{a}_z \cdot \nabla_t \times \tilde{J}_t^S$. Because the surface current density $\tilde{J}_t^S = \bar{a}_x J_x^S + \bar{a}_y J_y^S$ is zero outside the strip, one can again show that $\tilde{j}_+(\lambda)$ is analytic only in the upper half of the complex λ -plane.

In the next section, solution to the two Wiener Hopf equations will be discussed. We note that once $F_-(\lambda)$ is known, the reflection coefficient of the TEM in the waveguide can be obtained from the Fourier inverse transform of the scattered field component, $E_z^S(y; z)$. As evident from (7) and (10), the integral

$$E_z^S(y, z) = \int_{-\infty}^{\infty} (u_n \operatorname{sh} u_n k_0 d)^{-1} \operatorname{ch} u_n k_0 z \tilde{F}_-(\lambda) e^{-ik_0 \lambda y} d\lambda$$

can be enclosed in the lower half of the λ -plane for the parallel plate region, $y > 0$. Since $\tilde{F}_-(\lambda)$ is analytic in the lower half-plane, the reflection coefficient of the TEM wave is known from the residue contribution at $\lambda = (n^2 - \alpha^2)^{\frac{1}{2}}$ as

$$E_z^S(y, z) = \Gamma_{\text{TEM}} e^{-ik_0 (n^2 - \alpha^2)^{\frac{1}{2}} y}; \quad (16)$$

$$\Gamma_{\text{TEM}} = \pi i [k_0 d (n^2 - \alpha^2)^{\frac{1}{2}}]^{-1} \tilde{F}_-(\lambda = \sqrt{n^2 - \alpha^2}) \quad (17)$$

Together with the implicit dependence of $\exp(ik_0 \alpha x)$ in the x-direction, eq. (16) then corresponds to a reflected TEM wave propagating away from the edge at an angle equal to negative of the incidence angle ϕ . It is of interest to know that only \tilde{F}_- , but not \tilde{G}_- , is involved in the expression of Γ_{TEM} .

3. Spectral Solution $\tilde{F}_-(\lambda)$ and $\tilde{G}_-(\lambda)$

Formal expressions for \tilde{F}_- and \tilde{G}_- can be derived by employing the typical Wiener-Hopf procedure. First, we factorize the kernel functions Q_e and Q_m into positive and negative functions according to $Q = Q_+Q_-$ and $Q_+(\lambda) = Q_-(-\lambda)$, where Q_{\pm} is formally known as [Mitra and Lee, 1971]

$$Q_{\pm}(\lambda) = Q^{\frac{1}{2}}(0) \exp \left\{ \pm \frac{1}{2\pi i} \int_{C_{\pm}} \frac{Q'(w)}{Q(w)} \ln \left(\frac{w-\lambda}{w} \right) dw \right\} \quad (18)$$

and C_{\pm} is the integration path from $-\infty \mp i0$ to $+\infty \mp i0$ as shown in Fig. 2. After the splitting of $\rho_{-}^i Q_{e+}$ into the sum of a positive and a negative function, i.e.,

$$\rho_{-}^i Q_{e+} = \frac{i\epsilon_r}{2\pi} \left(\frac{1}{\lambda + \sqrt{n^2 - \alpha^2}} \right) Q_{e+}(-\sqrt{n^2 - \alpha^2}) + \frac{i\epsilon_r}{2\pi} \left\{ \frac{1}{\lambda + \sqrt{n^2 - \alpha^2}} \left[Q_{e+}(\lambda) - Q_{e+}(-\sqrt{n^2 - \alpha^2}) \right] \right\}_+ \quad (19)$$

One immediately obtains from (11), the following formal solution

$$\tilde{F}_-(\lambda) = \left(\frac{i\epsilon_r}{2\pi} \right) \left[C_1 - Q_{e+}(-\sqrt{n^2 - \alpha^2}) \frac{1}{\lambda + \sqrt{n^2 - \alpha^2}} \right] Q_{e-}(\lambda) \quad (20)$$

$$\tilde{\rho}_+^s(\lambda) = \frac{i\epsilon_r \epsilon_0}{2\pi} \left\{ C_1 + \frac{1}{\lambda + \sqrt{n^2 - \alpha^2}} \left[Q_{e+}(\lambda) - Q_{e+}(-\sqrt{n^2 - \alpha^2}) \right] \right\} Q_{e+}^{-1}(\lambda) \quad (21)$$

where C_1 is a yet-undetermined constant. We note that, in deriving (20) and (21) use has been made of the edge condition for $\rho_+^s(y)$ as $y \rightarrow 0_+$. Following essentially the same procedure, we can also obtain from (14) the formal solution of \tilde{G}_- and \tilde{j}_+ as

$$\tilde{G}_-(\lambda) = \left(\frac{\epsilon_r}{2\pi} \right) C_2 Q_{m-}(\lambda), \quad (22)$$

$$\tilde{j}_+(\lambda) = i \left(\frac{\omega \epsilon_0 \epsilon_r}{2\pi} \right) C_2 Q_{m+}^{-1}(\lambda) \quad (23)$$

the case of normal incident where $\alpha = 0$, can one then excite the LSE-wave with a vertical electric field component, without the LSM-waves. It is of interest to note that since the incident wave has no x-dependence in this case, the problem actually reduces to the two dimensional case previously investigated by Bates and Mittra, [1968]. The approach we used to obtain the solution also appears to be similar to the work of Fialkovskii [1976] and Nefedov and Fialkovskii [1977], although no description than how they obtained their result is documented.

4. Reflection Coefficient and End Admittance

For our later discussion, it is somewhat more convenient to define two new kernel functions

$$\hat{Q}_e(\lambda) = \left(\frac{\epsilon_r}{k_0}\right) \frac{u_0 \text{th } u_n k_0 d}{u_n (\epsilon_r u_0 + u_n \text{th } u_n k_0 d)} \quad (28)$$

$$\hat{Q}_m(\lambda) = \frac{1}{k_0 d (\mu_r u_0 + u_n \text{th } u_n k_0 d)} \quad (29)$$

so that

$$Q_e(\lambda) = \left(\frac{k_0 d}{\epsilon_r}\right) u_n^2 \hat{Q}_e(\lambda); \quad Q_m(\lambda) = (\mu_r k_0 d) \hat{Q}_m(\lambda) \quad (30)$$

At the low frequency limit, i.e. $k_0 d \rightarrow 0$, one can readily show by a small argument expansion of the hyperbolic functions that both \hat{Q}_e and \hat{Q}_m become unity, so that the leading terms in the original kernels now appear explicitly. Factorization of \hat{Q}_e and \hat{Q}_m can be carried out in the usual manner as indicated in (18):

$$\hat{Q}_+(\lambda) = \exp(-if/2); \quad f(\lambda) = i \ln \hat{Q}(0) + \frac{1}{\pi} \int_{C_+} \frac{\hat{Q}'(w)}{\hat{Q}(w)} \ln \left(\frac{w-\lambda}{w}\right) dw \quad (31)$$

for both subscript e and m. Now since the terms $(k_0 t u_n^2 / \epsilon_r)$ and $\mu_r k_0 t$ can be factorized by inspection, we obtain from (29) and (30), an alternative expression for the positive functions Q_{e+} and Q_m as follows:

$$Q_{e+}(\lambda) = i \left(\frac{k_0 d}{\epsilon_r} \right)^{\frac{1}{2}} (\sqrt{n^2 - \alpha^2} - \lambda) e^{-if_e(\lambda)/2} ; \quad Q_{m+}(\lambda) = (\mu_r k_0 t)^{\frac{1}{2}} e^{-if_m(\lambda)/2} \quad (32)$$

Using these expressions, we have derived in Appendix C the explicit form of $F_-(\lambda)$ as

$$F_-(\lambda) = \frac{-i}{\pi} k_0 d \sqrt{n^2 - \alpha^2} \left(\frac{\lambda + i\alpha \text{th} \Delta}{\sqrt{n^2 - \alpha^2} - i\alpha \text{th} \Delta} \right) e^{-i[f_e(-\lambda) - f_e(-\sqrt{n^2 - \alpha^2})]/2} \quad (33)$$

which, when substituted into (17) yields

$$\Gamma_{\text{TEM}} = e^{+i\chi(\alpha)} ; \quad \chi(\alpha) = 2 \tan^{-1} \left(\frac{\alpha}{\sqrt{n^2 - \alpha^2}} \text{th} \Delta \right) - f_e(-\sqrt{n^2 - \alpha^2}) \quad (34)$$

which agrees in form to the result obtained by Fialkovskii [1976]. One can also show that in the low frequency limit as $k_0 d \rightarrow 0$, $\chi(\alpha) \rightarrow 0$ and $\Gamma_{\text{TEM}} \rightarrow 1$, is also consistent with the result by Weinstein [1970]. Expressions are derived in Appendix C.

$$\Delta = \frac{\alpha}{\pi} \int_0^\infty \ln \left[\frac{u_n \epsilon_r}{u_n} \left(\frac{u_n + \mu_r u_0 \text{th} u_n k_0 d}{\epsilon_r u_0 + u_n \text{th} u_n k_0 d} \right) \right] \frac{d\lambda}{\lambda^2 + \alpha^2} , \quad (35)$$

$$f_e(-\sqrt{n^2 - \alpha^2}) = \tan^{-1} \left(\frac{n^2 - \alpha^2}{\alpha^2 - 1} \right)^{\frac{1}{2}} - \frac{2}{\pi} \sqrt{n^2 - \alpha^2} \int_0^\infty \ln \left[\frac{(1 + \epsilon_r) u_0^2 \text{th} u_n k_0 d}{u_n (\epsilon_r u_0 + u_n \text{th} u_n k_0 d)} \right] \frac{d\lambda}{\lambda^2 - (n^2 - \alpha^2)} \quad (36)$$

where the integral in (36) is defined as a principal-value integral at $\lambda = \sqrt{n^2 - \alpha^2}$. Recalling $u_0 = (\lambda^2 + \alpha^2 - 1)^{\frac{1}{2}}$, $u_n = (\lambda^2 + \alpha^2 - n^2)^{\frac{1}{2}}$, and $\text{Re } u_0 \geq 0$, after an integration-by-part, that the two integrands possess a pair of branch cuts at $\lambda = \pm i(\alpha^2 - 1)^{\frac{1}{2}}$ and a set of simple poles located at $\lambda = \pm \lambda_e$ where

$$\epsilon_r (\lambda_e^2 + \alpha^2 - 1)^{\frac{1}{2}} + (\lambda_e^2 + \alpha^2 - n^2)^{\frac{1}{2}} \text{th} (\lambda_e^2 + \alpha^2 - n^2)^{\frac{1}{2}} = 0 \quad \text{LSE mode} \quad (37a)$$

and an additional set of poles at $\lambda = \pm\lambda_m$ where

$$\mu_r(\lambda_m^2 + \alpha^2 - 1)^{\frac{1}{2}} + (\lambda_m^2 + \alpha^2 - n^2)^{\frac{1}{2}} \text{cth}(\lambda_m^2 + \alpha^2 - n^2)^{\frac{1}{2}} = 0, \quad \text{LSM-mode} \quad (37b)$$

in the case of the first integral. By setting $\lambda_e^2 + \alpha^2 = \alpha_p^2$ in (37a) and $\lambda_m^2 + \alpha^2 = \alpha_p^2$ in (37b), one immediately sees that these are the same characteristic equations for the LSE and LSM surface modes as we discussed at the beginning of this paper. Now since the value of $\alpha = n \sin \phi$ varies from 0 to n , depending upon the incident angle ϕ of the TEM-wave, location of these singularities and hence, the value of the two integrals can change accordingly. Assuming the thickness of the slab is such that only the LSE₁-mode can propagate, the path of integration relative to the location of these singularities, is depicted in Fig. 3 for three possible ranges of incident angle: (i) $1 < \alpha_p < \alpha < n$, (ii) $1 < \alpha < \alpha_p < n$; (iii) $\alpha < 1 < \alpha_p < n$. In the first case, u_0 is real and the integrand is not only real, but smoothly varying (except near $\lambda = \sqrt{n^2 - \alpha^2}$) along the path of integration. Hence, the value of Δ , $fe(-\sqrt{n^2 - \alpha^2})$ and consequently, $\chi(\alpha)$ are all real. The magnitude of Γ_{TEM} is therefore unity, and the incident power is completely reflected back. As we mentioned before, this situation is very similar to a plane-wave incident onto a dielectric interface beyond the critical angle. As in the case of a dielectric waveguide, the phenomenon certainly can be utilized to guide an electromagnetic wave along x-direction when the conducting strip is truncated and a transverse resonance is imposed. In a companion paper, we shall discuss the guided wave on a wide microstrip based on this concept. On the other hand, for the case (ii) when $1 < \alpha < \alpha_p$, a simple pole will appear on the positive real axis and the path of integration will have to be deformed upward as shown in Fig.3. Although the remaining integration still

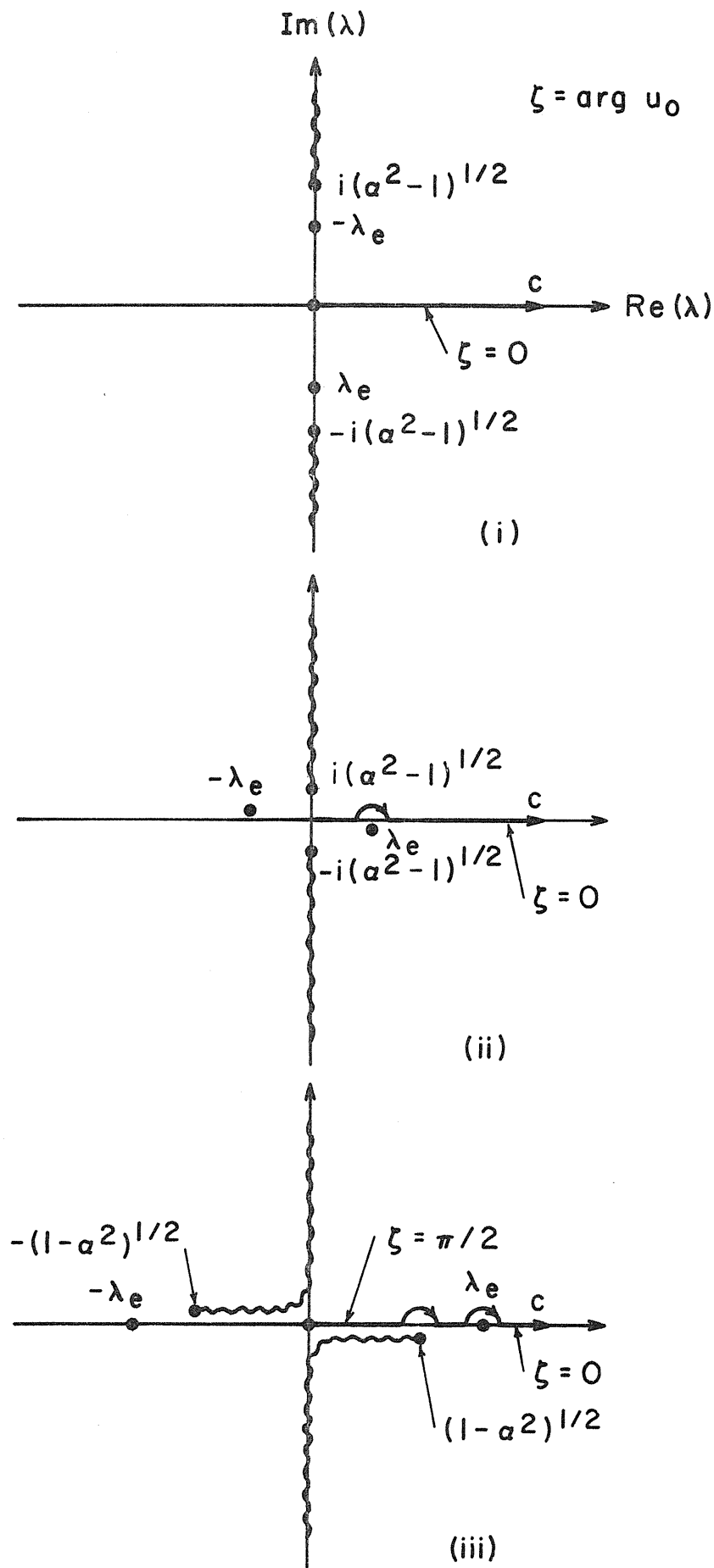


Figure 3

has a real value, it can be shown that the deformation around the pole yields an imaginary part equal to half the residue at $\lambda = \lambda_e$. As it will be demonstrated later in the numerical examples, the magnitude of Γ_{TEM} is now less unity, as part of the power is now used to excite the surface wave.

Finally, in case (iii) where $\alpha < 1 < \alpha_p$, the integrands in (35) and (36) are now complex for the integration range $0 < \lambda < (1-\alpha^2)^{\frac{1}{2}}$. The magnitude of Γ_{TEM} can be shown to be even smaller, since power can now radiate into the open region in the form of "sky-waves."

From the form of Γ_{TEM} in (34), one can also define the apparent end-admittance of such a structure as

$$Y_a(\alpha) = Y_c \frac{1-\Gamma_{\text{TEM}}}{1+\Gamma_{\text{TEM}}} = -iY_0 \tan[\chi(\alpha)/2] \quad (38)$$

where $Y_0 = (\eta_1 d)^{-1}$ ohm/m is the characteristic admittance of the TEM-wave in a parallel-plate waveguide. While numerical examples will be given later, it suffices to note that this admittance is a function of both frequency and angle of incidence.

5. Far Field and Surface-wave Radiation

Since the coefficients E_0 and H_0 are related directly to \tilde{F}_- and \tilde{G}_- , in (10), all the field components in the air region can be obtained by inverting the spectral solution given in (6). In particular, the far field can be shown asymptotically to be proportional to its spectral solutions with the substitution $\lambda = (1-\alpha^2)^{\frac{1}{2}} \cos \theta$ (or $-i(\alpha^2-1)^{\frac{1}{2}} \cos \theta$ for $\alpha > 1$). This is true, provided, of course, the observation point is not near the slab surface, or, in other words, the surface-wave pole, if it exists, is not close to the saddle-point. [Felsen and Marcuvitz, 1973].

For a fixed cross-section, we can show from (6) that the far-field variation is characterized by

$$\begin{pmatrix} E_x \\ \eta H_x \end{pmatrix} = \left(\frac{i4\pi I_0}{\sqrt{\alpha^2 - 1}} \right) \frac{1}{\alpha^2 \sin^2 \theta + \cos^2 \theta} \begin{pmatrix} \alpha \sin \theta & \cos \theta \\ -\cos \theta & \alpha \sin \theta \end{pmatrix} \begin{pmatrix} F(\lambda) \\ -i\sqrt{\alpha^2 - 1} \sin \theta G_-(\lambda) \end{pmatrix}_{\lambda = -i\sqrt{\alpha^2 - 1} \cos \theta}$$

where $\theta = \tan^{-1}(z/y)$; $r = (y^2 + z^2)^{\frac{1}{2}}$ and $I_0 = [-i/4 H_0^{(2)}(k_0 \sqrt{1 - \alpha^2} r)]$, as $k_0(1 - \alpha)^{\frac{1}{2}} r \gg 1$, is the far field of a line source. We note that since the radial component of both electric and magnetic fields have to vanish asymptotically in the far-field, it is more convenient to characterize the solution in the far-field region in terms of E_x and H_x . Furthermore, for incident angle ϕ greater than some critical angle $\phi_c = \sin^{-1}(1/n)$, the term $(1 - \alpha^2)^{\frac{1}{2}}$ is purely imaginary so that the far-field actually decays exponentially, rather than propagating away from the structure. If we now utilize the expression (C.4) and (C.5) derived in Appendix C for $F_-(\lambda)$ and $G_-(\lambda)$, we obtain the following expression

$$\begin{pmatrix} E_x \\ \eta_0 H_x \end{pmatrix} = \frac{A_0}{\alpha^2 \sin^2 \theta + \cos^2 \theta} \begin{pmatrix} \sin & \cos \theta \\ -\cos \theta & \alpha \sin \theta \end{pmatrix} \begin{pmatrix} \mathcal{F}_e(\theta; \alpha) \\ \mathcal{F}_m(\theta; \alpha) \end{pmatrix} \quad (39)$$

$$\mathcal{F}_e(\theta; \alpha) = (\sqrt{\alpha^2 - 1} \operatorname{ch} \Delta \cos \theta - \alpha \operatorname{sh} \Delta) \exp[-if_e(i\sqrt{\alpha^2 - 1} \cos \theta)]$$

and

$$\mathcal{F}_m(\theta; \alpha) = -i \sin \theta \alpha \sqrt{\alpha^2 - 1} \exp[-if_m(+i\sqrt{\alpha^2 - 1} \cos \theta)]$$

where $A_0 = -i4k_0 d \sqrt{\alpha^2 - 1} I_0 (\operatorname{ch} \Delta - i\alpha \operatorname{sh} \Delta / \sqrt{1 - \alpha^2})^{-1}$ is the amplitude of the two field strengths. Expression for f_e and f_m is again given in (C.6) and (C.7) in Appendix C. Obviously, as the operating frequency goes down, A_0 decreases continuously to zero as one would expect in the static limit.

where \tilde{j}_{t-}^i and $\tilde{\rho}_{-}^i$ can be obtained directly from (1) as

$$\tilde{\rho}_{-}^i = \left(\frac{i\epsilon_r \epsilon_0}{2\pi} \right) \left[\frac{1}{\lambda + (n^2 - \alpha^2)^{\frac{1}{2}}} \right]; \quad (B.5)$$

$$\tilde{j}_{t-}^i = \frac{i}{2\pi\eta_0 \mu_r} (\alpha \bar{a}_x - \sqrt{n^2 - \alpha^2} \bar{a}_y) \left[\frac{1}{\lambda + (n^2 - \alpha^2)^{\frac{1}{2}}} \right].$$

As it appears, the right-hand side of (B.4) has poles located at $\lambda = -\sqrt{n^2 - \alpha^2}$ and $i\alpha$ in the upper half of the complex α -plane. The pole at $\lambda = -\sqrt{n^2 - \alpha^2}$ is only a pseudo one since the contributions from $\tilde{\rho}_{-}^i$ and \tilde{j}_{t-}^i mutually cancel out. However, the pole at $\lambda = i\alpha$ can be eliminated only by enforcing a condition on $\tilde{\rho}_{+}^s$ and \tilde{j}_{+}^s so that

$$\{i\omega\alpha(\tilde{\rho}_{+}^s - \tilde{\rho}_{-}^i) + \lambda\tilde{j}_{+}^s\} = 0 \text{ and } \{i\omega\lambda(\tilde{\rho}_{+}^s - \tilde{\rho}_{-}^i) - \alpha\tilde{j}_{+}^s\}_{\lambda=i\alpha} = 0$$

or alternatively, $\omega(\tilde{\rho}_{+}^s - \tilde{\rho}_{-}^i) + \tilde{j}_{+}^s = 0$ at $\lambda = i\alpha$. Substitutions of the expression in (21) and (23) now yields the additional condition on C_1 and C_2 :

$$C_1 Q_{m+}(i\alpha) + C_2 Q_{e+}(i\alpha) = (\sqrt{n^2 - \alpha^2} + i\alpha)^{-1} Q_{e+}(-\sqrt{n^2 - \alpha^2}) Q_{m+}(i\alpha) \quad (B.6)$$

APPENDIX C

To obtain a suitable expression for $F_-(\lambda)$ and $G_-(\lambda)$, we first define

$$\Delta = -i[f_e(i\alpha) - f_m(i\alpha)]/2 \quad (C.1)$$

where f_e and f_m are given in (31), so that from (27) and (32),

$$\begin{aligned} \Omega_1 &= \frac{(\sqrt{n^2 - \alpha^2} - i\alpha)^2 - n^2 e^{-2\Delta}}{(\sqrt{n^2 - \alpha^2} - i\alpha)^2 + n^2 e^{-2\Delta}} = \frac{1 - \exp\{+i2(\tan^{-1} \alpha/\sqrt{n^2 - \alpha^2} + i\Delta)\}}{1 + \exp\{i2(\tan^{-1} \alpha/\sqrt{n^2 - \alpha^2} + i\Delta)\}} \\ &= -i \tan\left(\tan^{-1} \frac{\alpha}{\sqrt{n^2 - \alpha^2}} + i\Delta\right) \\ &= \frac{\alpha + i\sqrt{n^2 - \alpha^2} \operatorname{th} \Delta}{\sqrt{n^2 - \alpha^2} - i\alpha \operatorname{th} \Delta} \end{aligned} \quad (C.2)$$

Expression for Ω_2 can then be obtained from (C.2) and (27) as

$$\begin{aligned} \Omega_2 &= -i(1 - \Omega_1^2)^{\frac{1}{2}} = -i \sec\left(\tan^{-1} \frac{\alpha}{\sqrt{n^2 - \alpha^2}} + i\Delta\right) \\ &= \frac{-in}{\sqrt{n^2 - \alpha^2} \operatorname{ch} \Delta - i\alpha \operatorname{sh} \Delta} \end{aligned} \quad (C.3)$$

Substitution of (C.2) and (C.3) into (26) and (20) yields immediately the expression for $F_-(\lambda)$ as

$$\begin{aligned} F_-(\lambda) &= \frac{i\epsilon_r}{2\pi} \left\{ \frac{1}{n^2} \left(\frac{\sqrt{n^2 - \alpha^2} + \alpha^2 + i\alpha\sqrt{n^2 - \alpha^2} \operatorname{th} \Delta}{\sqrt{n^2 - \alpha^2} - i\alpha \operatorname{th} \Delta} \right) - \frac{1}{\lambda + \sqrt{n^2 - \alpha^2}} \right\} Q_e(\lambda) Q_{e+}(-\sqrt{n^2 - \alpha^2}) \\ &= \frac{-ik_0 d}{\pi} \sqrt{n^2 - \alpha^2} \left(\frac{\lambda + i\alpha \operatorname{th} \Delta}{\sqrt{n^2 - \alpha^2} - i\alpha \operatorname{th} \Delta} \right) e^{-i[f_e(-\lambda) + f_e(-\sqrt{n^2 - \alpha^2})]/2} \end{aligned} \quad (C.4)$$

and from (26) and (22), the expression for $G_-(\lambda)$ as

$$\begin{aligned} G_-(\lambda) &= \left(\frac{-\epsilon_r}{2\pi n} \right) \frac{\alpha}{\sqrt{n^2 - \alpha^2} \operatorname{ch}\Delta - i\alpha \operatorname{sh}\Delta} Q_{e+}(-\sqrt{n^2 - \alpha^2}) Q_{m-}(\lambda) \\ &= \frac{-i k_o d}{\pi} \sqrt{n^2 - \alpha^2} \left(\frac{\alpha}{\sqrt{n^2 - \alpha^2} \operatorname{ch}\Delta - i\alpha \operatorname{sh}\Delta} \right) e^{-i[f_e(\sqrt{n^2 - \alpha^2}) + f_m(-\lambda)]/2} \end{aligned} \quad (C.5)$$

We derive representations of Δ and $f_e(-\sqrt{n^2 - \alpha^2})$ convenient for computation. First, the form of \hat{Q}_e and \hat{Q}_m are rewritten as

$$\hat{Q}_e(\lambda) = \frac{\epsilon_r}{(1 + \epsilon_r) k_o d u_o} q_e(\lambda); \quad q_e = \frac{(1 + \epsilon_r) u_o^2 \operatorname{th} u_n k_o d}{u_n (\epsilon_r u_o + u_n \operatorname{th} u_n k_o d)}$$

$$\hat{Q}_m(\lambda) = \frac{1}{(1 + \mu_r) k_o d u_o} q_m(\lambda); \quad q_m = \frac{(1 + \mu_r) u_o}{\mu_r u_o + u_n \operatorname{cth} u_n k_o d}$$

so that the terms q_e and q_m approach unity as $|\lambda| \rightarrow \infty$. Splitting of these terms can then be done formally without introducing the value of the functions at $\lambda = 0$ as indicated in (18). Defining f_e and f_m in the same way as in (31), we have

$$f_e(\eta) = i \ln \left\{ \frac{\epsilon_r}{(1 + \epsilon_r) k_o d [\sqrt{\alpha^2 - 1} - i\eta]} \right\} + \frac{2\eta}{\pi} \int_0^\infty \ln q_e(\lambda) \frac{d\lambda}{\lambda^2 - \eta^2} \quad (C.6)$$

$$f_m(\eta) = i \ln \left\{ \frac{1}{(1 + \mu_r) k_o d [\sqrt{\alpha^2 - 1} - i\eta]} \right\} + \frac{2\eta}{\pi} \int_0^\infty \ln q_m(\lambda) \frac{d\lambda}{\lambda^2 - \eta^2} \quad (C.7)$$

which can be used to give the following expression for Δ :

$$\begin{aligned}
\Delta &= \frac{1}{2} \ln \frac{\epsilon_r (1 + \mu_r)}{1 + \epsilon_r} + \frac{\alpha}{\pi} \int_0^{\infty} \ln \left[\frac{u_o}{u_n} \left(\frac{1 + \epsilon_r}{1 + \mu_r} \right) \frac{u_n + \mu_r}{\epsilon_r u_o} \frac{u_o \operatorname{th} u_n k d}{u_n k d} \right] \frac{d\lambda}{\alpha^2 + \lambda^2} \\
&= \frac{\alpha}{\pi} \int_0^{\infty} \ln \frac{\epsilon_r u_o (u_n + \mu_r u_o \operatorname{th} u_n k d)}{u_n (\epsilon_r u_o + u_n \operatorname{th} u_n k d)} \frac{d\lambda}{\alpha^2 + \lambda^2} \tag{C.8}
\end{aligned}$$

Expression for $f_e(-\sqrt{n^2 - \alpha^2})$ is somewhat more complicated because $\lambda = \sqrt{n^2 - \alpha^2}$ is located slightly below the real axis. To ease any possible computational difficulty, we define the integral as a principal-value integral at $\lambda = \sqrt{n^2 - \alpha^2}$ by substrating the half residue at $\lambda = \sqrt{n^2 - \alpha^2}$. Consequently, we obtain

$$f_e(-\sqrt{n^2 - \alpha^2}) = -i \ln \frac{\sqrt{\alpha^2 - 1} + i\sqrt{n^2 - \alpha^2}}{\sqrt{n^2 - 1}} - \frac{2\sqrt{n^2 - \alpha^2}}{\pi} \int_0^{\infty} \ln q_e(\lambda) \frac{d\lambda}{\lambda^2 - (n^2 - \alpha^2)} \tag{C.9}$$